Supplementary Materials for: Mantle plumes are oxidized

Yves Moussallam[1,2], Marc-Antoine Longpré[3], Catherine McCammon[4], Alejandra Gomez-Ulla[1], Estelle F. Rose-Koga[1], Bruno Scaillet[5], Nial Peters[6], Emanuela Gennaro[7], Raphael Paris[1], Clive Oppenheimer[6]

[1] *Université Clermont Auvergne, CNRS, IRD, OPGC, Laboratoire Magmas et Volcans, F-63000 Clermont-Ferrand, France*

[2] *Lamont-Doherty Earth Observatory, Columbia University, New York, USA*

[3] *School of Earth and Environmental Sciences, Queens College, City University of New York, Queens, NY 11367, USA*

[4] *Bayerisches Geoinstitut, University of Bayreuth, D-95440 Bayreuth, Germany*

[5] *ISTO, UMR 7327, Université d'Orléans-CNRS-BRGM, 1A rue de la Férollerie, 45071 Orléans cedex 2, France*

[6] *Department of Geography, University of Cambridge, Downing Place, Cambridge, CB2 3EN, UK*

[7] *Istituto Nazionale di Geofisica e Vulcanologia, Sezione di Palermo, Via Ugo La Malfa, 153, 90146 Palermo, Italy*

Corresponding author: Yves Moussallam; yves.moussallam@gmail.com

Keywords: oxygen fugacity; degassing; XANES; Melt inclusions; plume

SUPPLEMENTARY FIGURES

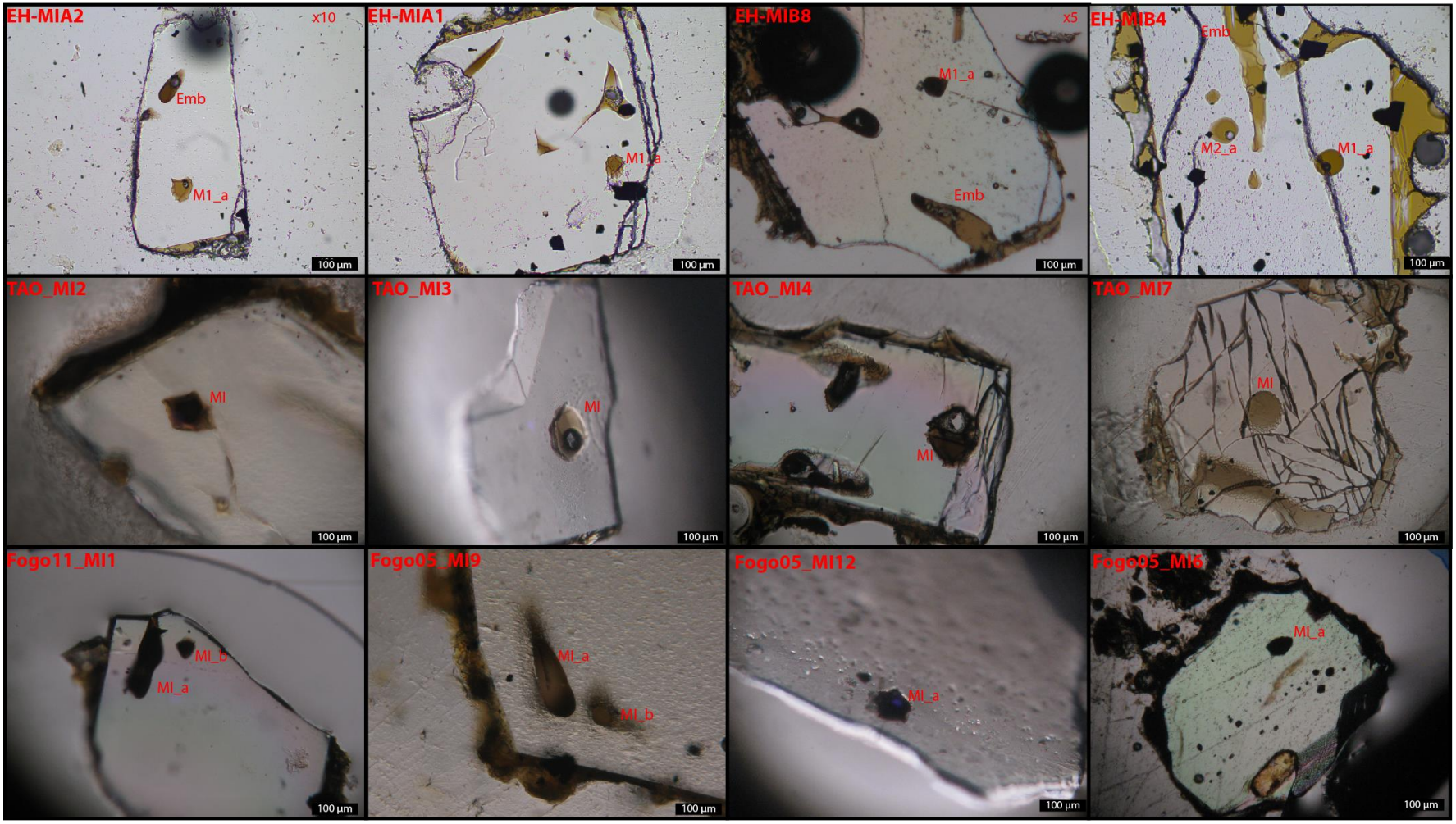

***Figure S1**: Transmitted light microphotographs of melt inclusions from El Hierro (top row), Lanzarote (central row), and Fogo (bottom row).*

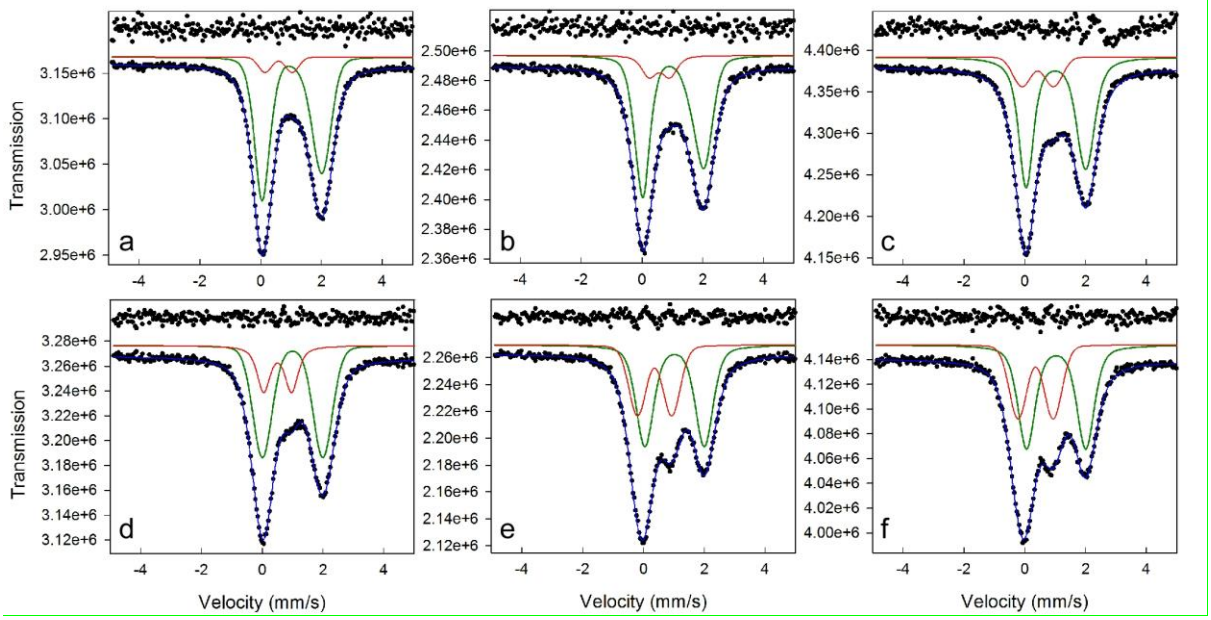

***Figure S2**: Room temperature Mössbauer spectra of the six basanitic standard glasses used in this study: (a) BAS_QFM_m1; (b) BAS_QFM; (c) BAS_NNO; (d) BAS_NNO_0.5; (e) BAS_NNO_1; (f) BAS_NNO_1.5. The green and red lines indicate the contributions from Fe^{2+} and Fe^{3+}, respectively. The fit residual is shown above each spectrum. $Fe^{3+}/\Sigma Fe$ ratios derived from relative areas corrected for recoil-free fraction effects according to Zhang et al. (2018) are given in Table S3.*

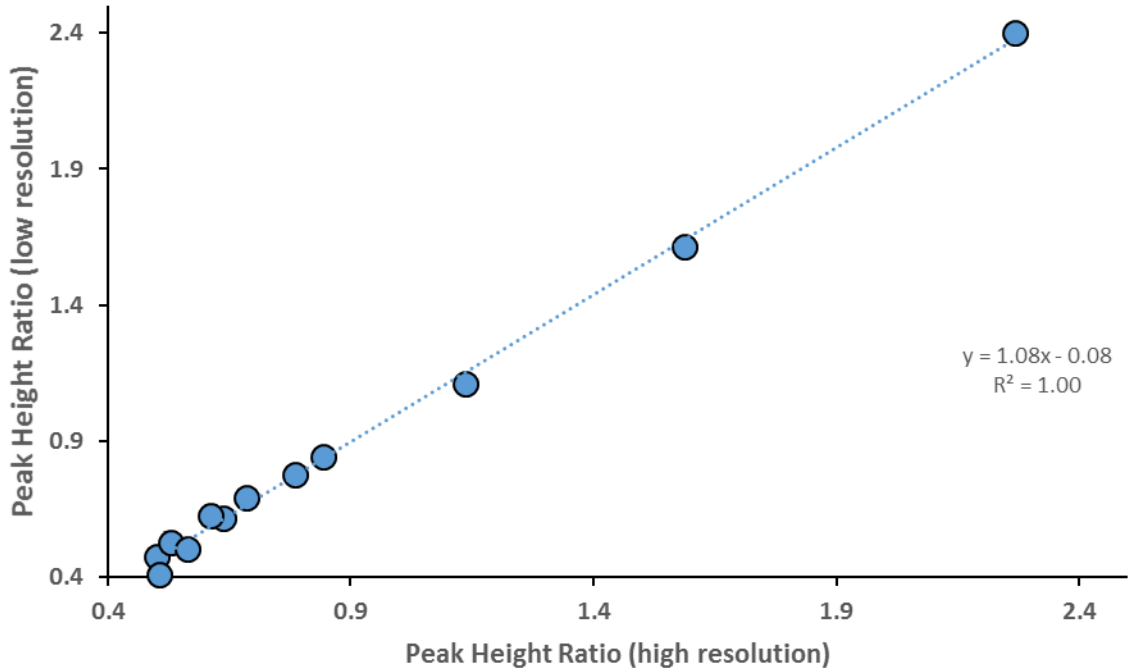

Figure S3: *Comparison between peak height ratios obtained from two co-added low resolution (0.25 mm Al plate attenuation) and from one high resolution (0.1 mm Al plate attenuation) XANES spectra.*

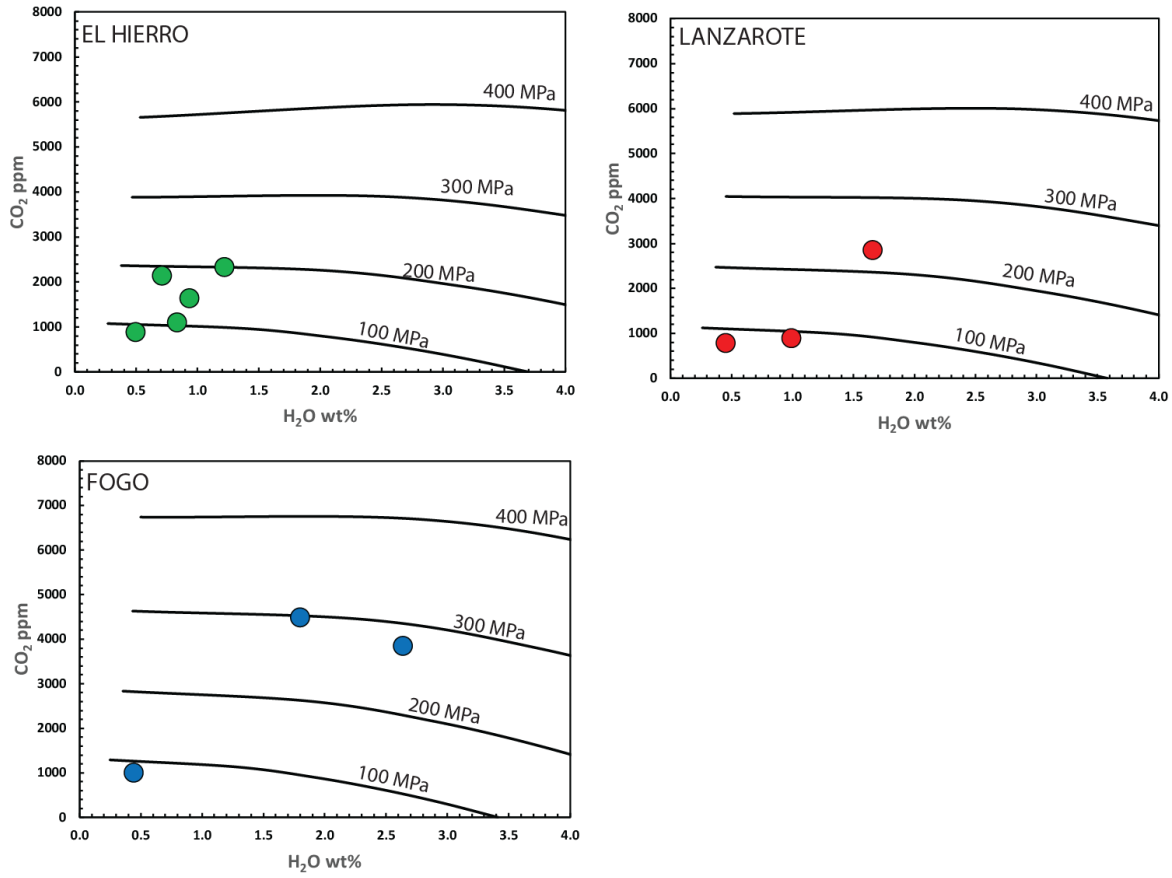

Figure S4: *CO_2-H_2O saturation curves between 100 and 400 MPa calculated with the model of* Iacono-Marziano et al., (2012*) for El Hierro, Lanzarote and Fogo melt compositions. Corresponding melt inclusions are shown as filled circle symbols.*

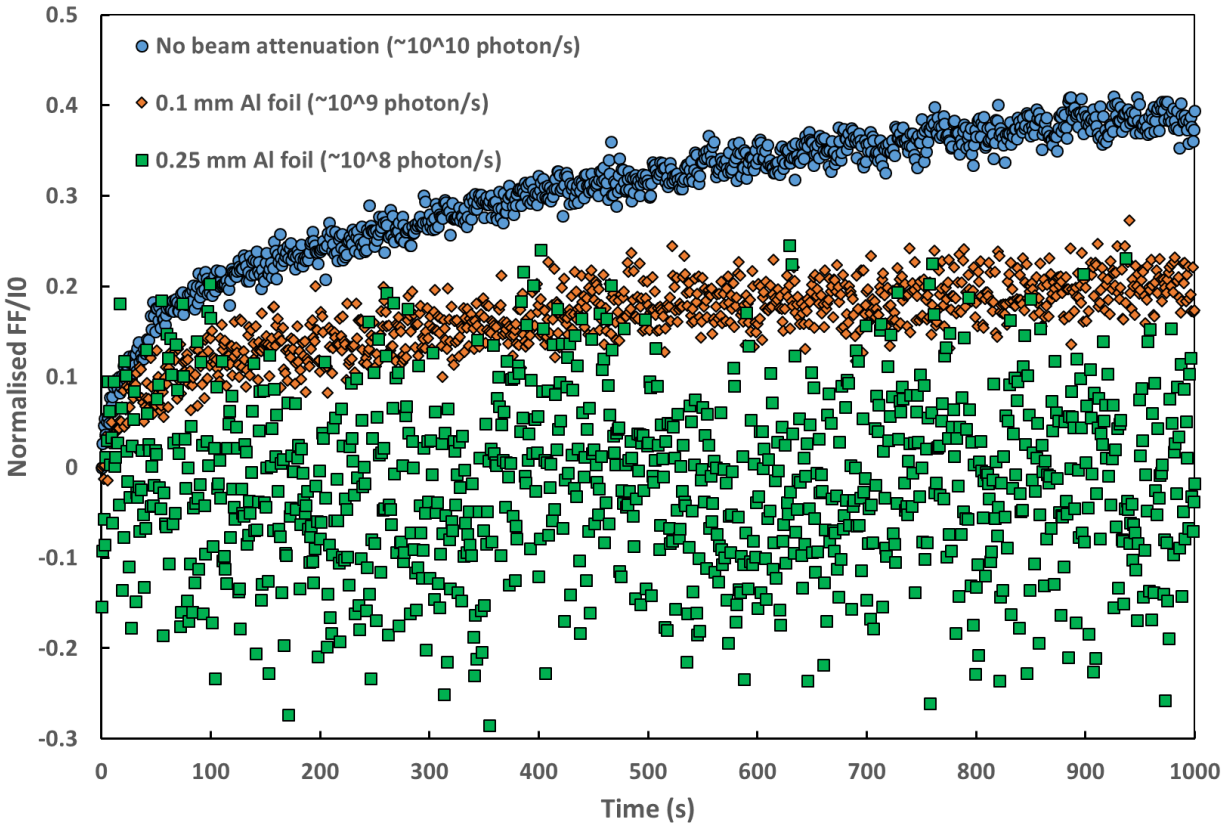

41

42 **Figure S5**: *Same data as Fig. 1 in main text (section 2.2) but without changing the detector*

43 *position between each attenuation conditions.*

44

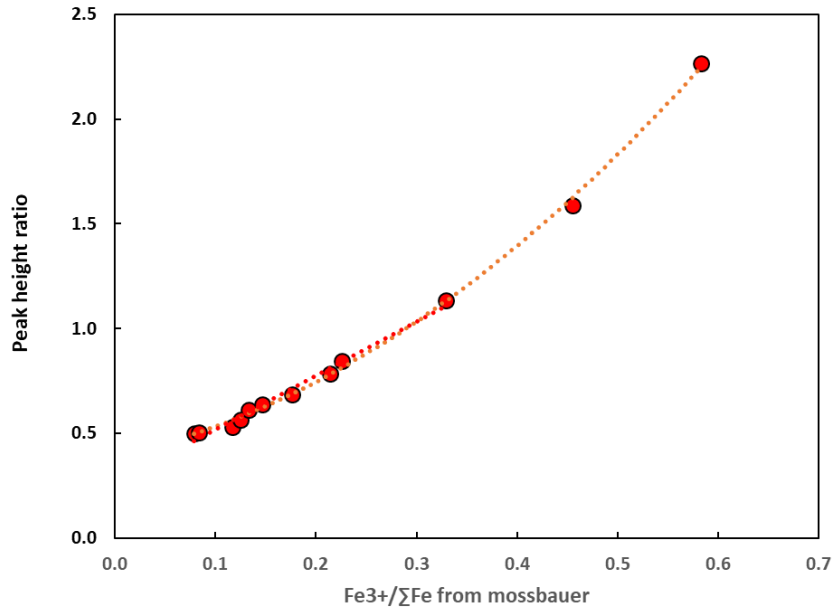

Figure S6: *Calibration line of the peak height ratio determined by XANES compared with the $Fe^{3+}/\sum Fe$ ratios determined by Mössbauer spectroscopy in basaltic standard glasses from the Smithsonian (Mössbauer $Fe^{3+}/\sum Fe$ values from* Zhang et al., 2018*). The figure shows that for $Fe^{3+}/\sum Fe$ ratios between 0.1 and 0.4, the relationship between peak height and $Fe^{3+}/\sum Fe$ is well captured by a linear regression.*

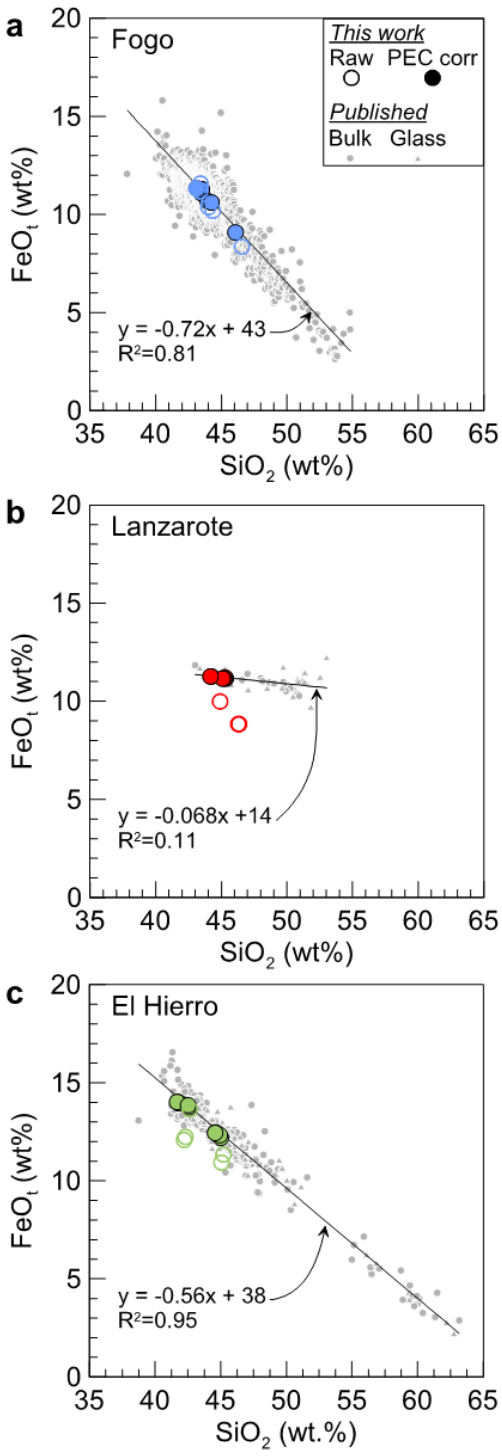

Figure S7: *Alternative method of iron loss assessment. Grey symbols show published bulk rock and glass compositions defining FeO_t–SiO_2 liquid lines of descent at (a) Fogo, (b) Lanzarote, and (c) El Hierro. The equations of linear fits through these data are given with their correlation coefficients (R^2) and can be used to estimate initial total iron content of melt*

inclusions based on measured SiO_2 content. Open and solid colored circles show uncorrected and corrected (PEC corr, accounting for iron-loss) melt inclusion compositions, respectively.

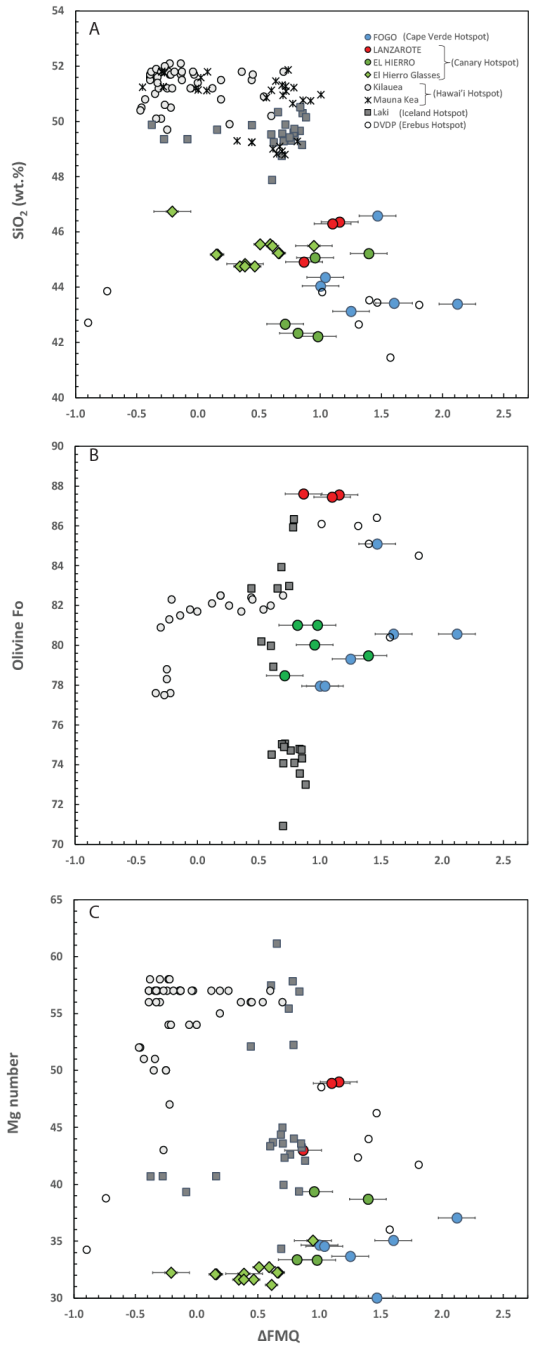

Figure S8: *Plot of various proxies of differentiation versus melt fO_2: A. SiO_2 content of the melt, B. Forsterite content of the olivine and C. Magnesium number of the melt (using FeO_t values). The absence of correlation between these proxies for differentiation and the oxidation*

state of the melt shows that there is no obvious change in melt oxidation state with differentiation.

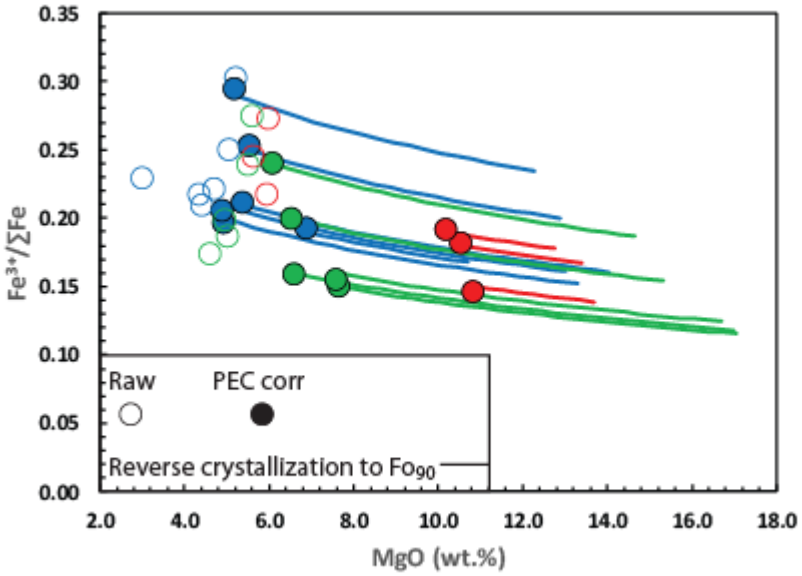

Figure S9: *Sensitivity analysis of the effects of post-entrapment crystallisation and pre-entrapment crystallization of olivine on melt* $Fe^{3+}/\sum Fe$. *Post-entrapment crystallisation estimated using Petrolog3 software (Danyushevsky and Plechov, 2011) and accounting for iron-loss as estimated by Fig. S7, assuming a system closed to oxygen, with* Fe^{3+} *behaving incompatibly. The effect of pre-entrapment crystallization of olivine is modelled with PRIMELT3* (Herzberg and Asimow, 2015) *until melt–*Fo_{90} *olivine equilibrium is reached.*

SUPPLEMENTARY TABLES

Table S1: Measured oxidation state and calculated oxygen fugacity of melt inclusions, embayment and glasses

Volcano	Sample name	Sample Type	MI minimum size long axis (μm)	$Fe^{3+}/\sum Fe$	1σ	Peak Ratio	1σ	Centroid energy	1σ	Delta FMQ
LANZAROTE	TAO_MI2_a_a	MI	87	0.27	0.012	0.99	0.03			**1.2**
	TAO_MI3_a_a	MI	106	0.22	0.012	0.84	0.03			**1.1**
	TAO_MI7_a_a	MI	78	0.17	0.012	0.70	0.03			**-0.2**
	TAO_MI4_a_a	MI	112	0.25	0.012	0.91	0.03			**0.9**
FOGO	Fogo11_MI1_a	MI	151	0.30	0.012	1.07	0.03			**2.1**
	Fogo11_MI1_b	MI	42	0.25	0.012	0.93	0.03			**1.6**
	Fogo05_MI9_a	MI	181	0.21	0.012	0.82	0.03			**1.0**
	Fogo05_MI9_b	MI	77	0.22	0.012	0.84	0.03			**1.0**
	Fogo05_MI12_a_a	MI	72	0.23	0.012	0.87	0.03			**1.5**
	Fogo05_MI6_a_a	MI	55	0.22	0.012	0.85	0.03			**1.3**
EL HIERRO	EH_MIB4_M1_a	MI	62	0.19	0.012	0.75	0.03			**0.8**
	EH_MIB4_M2_a	MI	61	0.20	0.012	0.79	0.03			**1.0**
	EH_MIB8_M1_a	MI	48	0.17	0.012	0.72	0.03			**0.7**
	EH_MIA1_M1_a	MI	36	0.27	0.012	0.99	0.03			**1.4**
	EH_MIA2_M1_a	MI	41	0.24	0.012	0.90	0.03			**1.0**
	EH_MIB4_Emb	Emb		0.16	0.012	0.69	0.03			**0.4**
	EH_MIB8_Emb	Emb		0.15	0.012	0.66	0.03			**-0.2**
	EH_MIA2_Emb	Emb		0.23	0.012	0.88	0.03			**0.9**

C1†	Glass	0.17	0.004	7113.4076	0.011	**0.1**
C2†	Glass	0.17	0.004	7113.3918	0.011	**0.0**
C3†	Glass	0.18	0.004	7113.4278	0.011	**0.1**
C4†	Glass	0.18	0.004	7113.4261	0.011	**0.1**
C7†	Glass	0.18	0.004	7113.4138	0.011	**0.1**
C8†	Glass	0.15	0.004	7113.3300	0.011	**-0.4**
C9†	Glass	0.15	0.004	7113.3282	0.011	**-0.4**
C10†	Glass	0.16	0.004	7113.3584	0.011	**-0.2**
C11†	Glass	0.16	0.004	7113.3805	0.011	**-0.1**
C12†	Glass	0.16	0.004	7113.3657	0.011	**-0.2**

77

78

79 **Table S2**: Acquisition parameters used during Fe K-edge XANES analysis
80

Energy range (eV)	Step size (eV)	Dwell time (s)
7020.0–7100.0	10	0.25
7101.0–7104.0	1	1
7104.1–7109.9	0.5	5
7110.0–7117.9	0.1	5
7118.0–7119.4	0.1	1
7119.5–7127.0	0.5	1
7128.0–7144.0	1	1
7148.0–7408.0	5	1
7410.0–7500.0	10	0.5

81

82

Table S3: $Fe^{3+}/\Sigma Fe$, centroid energies and peak height ratios for basanitic (this study) and basaltic (Smithsonian) standard glasses.

Standard	$Fe^{3+}/\sum Fe$ (Mössbauer)	error on $Fe^{3+}/\sum Fe$ (Mössbauer)	Peak Ratio	Centroid energy
BAS_QFM_m1	0.08	0.04	0.525	7113.015
BAS_QFM	0.13	0.04	0.638	7113.147
BAS_NNO	0.18	0.08	0.748	7113.248
BAS_NNO_0.5	0.22	0.04	0.776	7113.293
BAS_NNO_1	0.34	0.04	1.182	7113.687
BAS_NNO_1.5	0.34	0.03	1.211	7113.707
Smithsonian standards from Cottrell et al. (2009), modified by Zhang et al. (2018):				
LW_-20	0.079	0.006	0.499	7113.013
AII_-15	0.084	0.005	0.506	7113.019
LW_-10	0.117	0.005	0.529	7113.054
AII_-05	0.125	0.004	0.563	7113.062
LW_0	0.147	0.003	0.638	7113.157
AII_0	0.133	0.004	0.612	7113.128
AII_05	0.176	0.004	0.685	7113.209
LW_10	0.214	0.004	0.785	7113.318
AII_15	0.226	0.004	0.843	7113.381
AII_25	0.329	0.005	1.136	7113.674
AII_35	0.455	0.004	1.586	7113.945
AII_45	0.583	0.005	2.266	7114.166

Table S4: Measured volatile contents and calculated entrapment pressures (using the model of Iacono-Marziano et al., (2012)) of melt inclusions, embayment and glasses

Volcano	Sample name	Sample Type	P (MPa)*	H_2Ot	1σ estimated at 15%	CO_2(ppm)	1σ estimated at 15%	Cl	1σ	S	1σ	F	1σ
LANZAROTE	TAO_MI2_a_a	MI	90	0.5	0.1	796	119	1036	25	3020	104	1164	350
	TAO_MI3_a_a	MI	275	1.7	0.2	2858	429	929	25	2836	82	949	401
	TAO_MI7_a_a	MI		0.3	0.0								
	TAO_MI4_a_a	MI	103	1.0	0.1	899	135	1128	59	2693	119	1427	170
FOGO	Fogo11_MI1_a	MI	287	2.6	0.4	3854	578	1092	51	3603	106	1833	325
	Fogo11_MI1_b	MI		0.5	0.1			1078.2	32	3804	52	1720	151
	Fogo05_MI9_a	MI		1.6	0.2			1144.8	66	1932	78	2525	239
	Fogo05_MI9_b	MI		1.2	0.2			1108.2	43	1359	25	2449	239
	Fogo05_MI12_a_a	MI	277	1.8	0.3	4487	673	525.4	31	2996	96	1368	207
	Fogo05_MI6_a_a	MI	87	0.4	0.1	1005	151						
EL HIERRO	EH_MIB4_M1_a	MI	176	0.9	0.1	1650	248	944	79	2671	75	1403	347
	EH_MIB4_M2_a	MI	213	0.7	0.1	2151	323	926.4	65	2312	64	1713	295
	EH_MIB8_M1_a	MI						942.2	28	2503	70	1871	321
	EH_MIA1_M1_a	MI	125	0.8	0.1	1108	166	1004.6	35	3682	93	1286	282
	EH_MIA2_M1_a	MI	246	1.2	0.2	2332	350	913.4	47	3135	27	1421	224
	EH_MIB4_Emb	Emb		0.5	0.1			987.4	32	648	49	1817	378
	EH_MIB8_Emb	Emb	100	0.5	0.1	888	133	962.2	77	361	43	1669	302
	EH_MIA2_Emb	Emb						348.6	43	1821	56	1014	487
	C1†	Glass		0.7	0.0	428	153	934	57	417	24	1819	135

C2†	Glass	0.7	0.0	428	153	934	57	417	24	1819	135
C3†	Glass	1.0	0.0	155	19	1012	62	1033	63	1924	142
C4†	Glass	1.0	0.0	155	19	1012	62	1033	63	1924	142
C7†	Glass	0.5	0.0	49	8	1024	63	470	27	2136	158
C8†	Glass	0.4	0.0	61	10	995	62	443	26	2091	155
C9†	Glass	0.4	0.0	61	10	995	62	443	26	2091	155
C10†	Glass	0.5	0.0	84	28	977	61	560	32	2097	155
C11†	Glass	0.5	0.0	84	28	977	61	560	32	2097	155
C12†	Glass	0.5	0.0	84	28	977	61	560	32	2097	155

87 † Volatile data from average values in Longpré et al., (2017)

88

89 **Table S5:** Measured major element compositions of melt inclusions, embayment and glasses

Volcano	Sample name	Sample Type	SiO_2	TiO_2	Al_2O_3	FeO	MnO	CaO	MgO	Na_2O	K_2O	P_2O_5	Total	Mg# (Mg/Mg+Fe^{2+})	Mg# (Mg/Mg+FeOt)
LANZAROTE	TAO_MI2_a_a	MI	44.2	3.2	14.5	8.4	0.2	13.3	5.7	3.3	1.4	1.1	95.3	64	55
	TAO_MI3_a_a	MI	44.6	3.0	14.7	8.5	0.2	13.4	5.7	3.8	1.4	1.0	96.3	62	55
	TAO_MI7_a_a	MI													
	TAO_MI4_a_a	MI	43.9	3.1	16.0	9.7	0.2	10.7	5.5	5.2	1.7	1.6	97.7	58	50
FOGO	Fogo11_MI1_a	MI	41.8	3.6	15.7	10.8	0.2	11.5	5.0	3.5	2.9	1.3	96.4	56	45
	Fogo11_MI1_b	MI	41.9	3.6	16.0	11.2	0.2	11.3	4.9	3.4	2.9	1.2	96.6	52	44
	Fogo05_MI9_a	MI	45.3	3.8	17.6	10.7	0.2	12.1	4.6	4.6	3.0	1.1	102.9	50	43
	Fogo05_MI9_b	MI	45.5	3.8	17.7	10.4	0.2	10.7	4.5	4.9	3.3	1.5	102.5	51	43
	Fogo05_MI12_a_a	MI	45.7	3.5	16.8	8.2	0.4	14.0	3.0	3.1	2.9	0.6	98.2	47	39
	Fogo05_MI6_a_a	MI	41.6	3.6	15.9	10.9	0.2	12.4	4.5	3.7	2.6	1.0	96.5	50	43
EL HIERRO	EH_MIB4_M1_a	MI	41.8	5.2	15.0	12.1	0.1	12.8	5.0	4.1	1.6	1.1	98.6	48	42
	EH_MIB4_M2_a	MI	41.1	5.3	15.0	11.8	0.2	12.6	4.8	4.2	1.5	1.0	97.4	49	42
	EH_MIB8_M1_a	MI	42.0	5.3	15.1	13.4	0.3	11.3	4.5	4.0	1.5	1.0	98.5	43	38
	EH_MIA1_M1_a	MI	42.7	4.1	14.7	10.7	0.1	10.3	5.3	3.9	1.6	1.1	94.4	56	47
	EH_MIA2_M1_a	MI	43.8	5.1	14.7	10.6	0.0	12.1	5.4	3.3	1.4	0.8	97.3	55	47
	EH_MIB4_Emb	Emb	44.2	4.7	16.1	11.3	0.2	10.1	4.4	4.5	1.9	1.1	98.6	46	41
	EH_MIB8_Emb	Emb	48.6	4.5	17.5	11.1	0.1	9.6	4.4	5.0	2.0	1.1	103.9	46	41

EH_MIA2_Emb	Emb	44.1	4.4	15.1	11.2	0.1	10.8	4.9	3.7	1.6	1.0	97.0	51	44
C1†	Glass	45.1	4.3	15.4	11.9	0.2	10.8	4.8	4.7	1.7	1.1	99.1	48	42
C2†	Glass	45.1	4.3	15.4	11.9	0.2	10.8	4.8	4.7	1.7	1.1	99.1	47	42
C3†	Glass	44.8	4.5	15.2	11.9	0.2	11.2	4.7	4.6	1.7	1.1	99.2	47	41
C4†	Glass	44.8	4.5	15.2	11.9	0.2	11.2	4.7	4.6	1.7	1.1	99.2	47	41
C7†	Glass	45.2	4.3	15.5	12.0	0.2	10.3	4.5	4.9	2.0	1.1	99.3	46	40
C8†	Glass	44.9	4.4	15.5	12.0	0.2	10.4	4.7	4.9	1.9	1.1	99.3	46	41
C9†	Glass	44.9	4.4	15.5	12.0	0.2	10.4	4.7	4.9	1.9	1.1	99.3	46	41
C10†	Glass	44.6	4.7	15.5	12.3	0.2	10.2	4.7	4.9	2.0	1.1	99.6	46	41
C11†	Glass	44.6	4.7	15.5	12.3	0.2	10.2	4.7	4.9	2.0	1.1	99.6	46	41
C12†	Glass	44.6	4.7	15.5	12.3	0.2	10.2	4.7	4.9	2.0	1.1	99.6	46	41

90 † Composition data from average values in Longpré et al., (2017)

91

92 **Table S6:** Measured major element compositions of olivine host

Volcano	*Sample name*	*Sample Type*	*SiO_2*	*TiO_2*	*Al_2O_3*	*FeO*	*MnO*	*CaO*	*MgO*	*Total*	*Fo %*
LANZAROTE	TAO_MI2_a_a	MI	39.9	0.0	0.1	11.9	0.2	0.2	46.9	99.4	87.6
	TAO_MI3_a_a	MI	40.4	0.0	0.0	12.1	0.1	0.2	47.2	100.3	87.5
	TAO_MI7_a_a	MI									
	TAO_MI4_a_a	MI	39.7	0.0	0.1	11.8	0.1	0.2	47.0	99.3	87.6
FOGO	Fogo11_MI1_a	MI	39.9	0.0	0.0	18.0	0.2	0.3	41.8	100.4	80.6
	Fogo11_MI1_b	MI	39.9	0.0	0.0	18.0	0.2	0.3	41.8	100.4	80.6
	Fogo05_MI9_a	MI	41.3	0.1	0.1	18.4	0.3	0.3	36.4	97.0	77.9
	Fogo05_MI9_b	MI	41.3	0.1	0.1	18.4	0.3	0.3	36.4	97.0	77.9
	Fogo05_MI12_a_a	MI	41.6	0.0	0.0	13.5	0.2	0.4	43.1	98.9	85.1
	Fogo05_MI6_a_a	MI	39.5	0.0	0.1	19.0	0.3	0.3	40.9	100.1	79.3
EL HIERRO	EH_MIB4_M1_a	MI	39.4	0.1	0.1	17.7	0.2	0.2	42.4	100.3	81.0
	EH_MIB4_M2_a	MI	39.4	0.1	0.1	17.7	0.2	0.2	42.4	100.3	81.0
	EH_MIB8_M1_a	MI	39.5	0.0	0.0	19.8	0.2	0.2	40.5	100.4	78.5
	EH_MIA1_M1_a	MI	39.7	0.0	0.0	18.5	0.2	0.3	40.3	99.3	79.5
	EH_MIA2_M1_a	MI	39.7	0.2	0.0	18.0	0.2	0.3	40.4	98.7	80.0

93

94

Table S7: Post-entrapment crystallisation corrected compositions (see main text section 2.6.1 for details)

Sample name	*FO_CALC_Initial*	*SiO_2*	*TiO_2*	*Al_2O_3*	*Fe_2O_3*	*FeO*	*MnO*	*MgO*	*CaO*	*Na_2O*	*K_2O*	*P_2O_5*	*OL_PER*	*MELT_PER*
TAO_MI2_a_a	85.44	46.69	3.47	15.50	2.60	5.17	0.22	6.02	14.22	3.48	1.46	1.18	1.19	98.81
TAO_MI3_a_a	84.29	46.74	3.22	15.69	2.11	5.19	0.17	6.00	14.32	4.02	1.44	1.10	1.84	98.16
TAO_MI7_a_a														
TAO_MI4_a_a	82.32	45.54	3.36	17.13	2.78	4.80	0.21	5.61	11.49	5.53	1.84	1.74	3.45	96.55
Fogo11_MI1_a	81.52	43.31	3.73	16.13	3.59	7.97	0.17	5.22	11.89	3.64	3.04	1.32	-0.59	100.59
Fogo11_MI1_b	79.03	43.62	3.79	16.77	3.15	7.67	0.22	5.07	11.82	3.56	3.04	1.30	0.93	99.07
Fogo05_MI9_a	76.70	43.92	3.69	17.14	2.50	7.85	0.22	4.45	11.81	4.50	2.88	1.04	0.70	99.30
Fogo05_MI9_b	76.36	44.29	3.75	17.43	2.54	7.44	0.16	4.35	10.53	4.81	3.20	1.50	0.92	99.08
Fogo05_MI12_a_a	73.65	47.29	3.70	17.83	2.17	3.50	0.47	3.27	14.81	3.33	3.03	0.60	2.93	97.07
Fogo05_MI6_a_a	77.99	43.31	3.82	16.66	2.72	7.93	0.21	4.73	12.98	3.91	2.70	1.04	0.74	99.26
EH_MIB4_M1_a	77.07	42.70	5.43	15.73	2.59	7.93	0.15	5.10	13.34	4.24	1.67	1.13	2.44	97.56
EH_MIB4_M2_a	77.68	42.57	5.56	15.81	2.68	7.86	0.17	5.03	13.26	4.40	1.58	1.11	2.03	97.97
EH_MIB8_M1_a	72.35	43.26	5.63	16.07	2.72	8.30	0.33	4.75	11.99	4.27	1.63	1.06	3.66	96.34
EH_MIA1_M1_a	81.00	45.16	4.27	15.37	3.23	8.54	0.09	5.61	10.83	4.07	1.71	1.12	-1.05	101.05
EH_MIA2_M1_a	80.48	45.02	5.19	15.04	2.82	8.30	0.04	5.51	12.42	3.42	1.44	0.81	-0.28	100.28

98 **Table S8:** Pre-entrapment crystallisation compositions calculated to equilibrium with Fo_{90} (see main text section 2.7 for details)

Sample Name	$Fe^{3+}/\Sigma Fe$	%ol addition	SiO_2	TiO_2	Al_2O_3	Fe_2O_3	FeO	MnO	MgO	CaO	Na_2O	K_2O	P_2O_5
TAO_MI2_a_a	0.30	3	46.5	3.4	15.0	2.5	5.3	0.2	7.2	13.8	3.4	1.4	1.1
TAO_MI3_a_a	0.26	3	46.6	3.1	15.2	2.0	5.3	0.2	7.2	13.9	3.9	1.4	1.1
TAO_MI4_a_a	0.33	2	45.4	3.3	16.8	2.7	4.9	0.2	6.4	11.3	5.4	1.8	1.7
Fogo11_MI1_a	0.23	19	42.7	3.1	13.4	3.0	8.8	0.2	12.3	9.9	3.0	2.5	1.1
Fogo11_MI1_b	0.22	19	43.0	3.2	13.9	2.6	8.5	0.2	12.2	9.8	2.9	2.5	1.1
Fogo05_MI9_a	0.17	21	43.2	3.0	13.9	2.0	8.9	0.2	12.3	9.7	3.6	2.3	0.8
Fogo05_MI9_b	0.18	19	43.6	3.1	14.4	2.1	8.4	0.2	11.5	8.8	4.0	2.6	1.2
Fogo05_MI12_a_a	0.33	4	47.0	3.6	17.1	2.1	3.8	0.5	4.9	14.3	3.2	2.9	0.6
Fogo05_MI6_a_a	0.18	21	42.7	3.1	13.5	2.2	8.9	0.2	12.5	10.6	3.2	2.2	0.8
EH_MIB4_M1_a	0.18	19	42.2	4.5	13.0	2.1	8.7	0.2	12.2	11.1	3.5	1.4	0.9
EH_MIB4_M2_a	0.19	19	42.1	4.6	13.1	2.2	8.7	0.2	12.2	11.0	3.6	1.3	0.9
EH_MIB8_M1_a	0.17	23	42.6	4.5	12.8	2.2	9.3	0.3	13.1	9.6	3.4	1.3	0.8
EH_MIA1_M1_a	0.20	22	44.2	3.5	12.4	2.6	9.4	0.1	13.6	8.8	3.3	1.4	0.9
EH_MIA2_M1_a	0.18	21	44.1	4.2	12.2	2.3	9.2	0.0	13.2	10.1	2.8	1.2	0.7

99